Fatigue Crack Paths under Complex Loading

H.A. Richard[1], M. Sander[1] and M. Fulland[1]

[1] Institute of Applied Mechanics, University of Paderborn, Pohlweg 47-49,
33098 Paderborn, Germany, e-mail: richard@fam.upb.de

ABSTRACT. *In many cases the lifetime of technical structures and components depends on the behaviour of cracks. Due to complex geometry and loading situations in real-world-structures cracks are often subjected to superimposed normal, in-plane and out-of-plane stresses. This paper deals with experimental investigations and numerical simulations of fatigue crack growth under complex loading. In contrast to a pure Mode I loading, where the crack grows self-similar (coplanar) from the starter crack, the growth of Mixed Mode loaded cracks generally leads to non-planar crack surfaces. Experimentally and numerically determined fatigue crack paths in specimen and structures under complex loading will be described in the following.*

FATIGUE CRACK GROWTH IN REAL STRUCTURES

In many cases fatigue crack growth leads to failure of components and structures. This is documented by serious accidents of aircrafts (Figure 1), ships or railways, but also by numerous fatigue cracks in technical components in machines. The origin of such damages are imperfections or cracks, which initially grow stable as a result of the service loading. In many cases these cracks are subjected to complex loading situations, so called Mixed Mode loadings, which result from the geometry and/or the external loading of the component.

Figure 1. Fatigue crack growth in an aircraft structure.

Figure 2a presents a structure, whose cracks generally are exposed to a plane Mixed Mode loading. The local loading conditions at the crack tip are characterised by the stress intensity factors K_I and K_{II}, which show in case of quasi-static loading the same time-dependency the applied stress $\sigma(t)$.
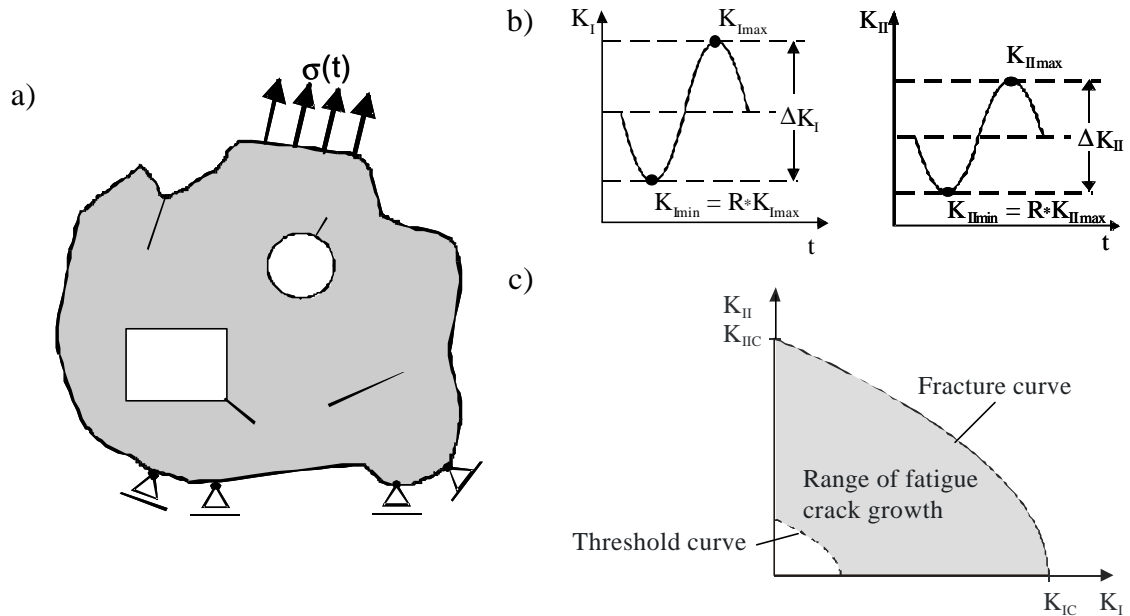
Figure 2. a) Mixed Mode cracks in a structure
b) Stress intensity factors $K_I(t)$ and $K_{II}(t)$ at a mixed mode crack
c) K_I/K_{II}-diagram with the range of fatigue crack growth.

The fatigue crack growth is governed the cyclic stress intensity factors ΔK_I und ΔK_{II} (Figure 2b) respectively the cyclic comparative stress intensity factor ΔK_V, which is determined by [1, 2]

$$\Delta K_V = \frac{\Delta K_I}{2} + \frac{1}{2}\sqrt{\Delta K_I^2 + 6\Delta K_{II}^2} \qquad (1).$$

Fatigue crack growth is possible, if ΔK_V exceeds the threshold value ΔK_{th} for Mode I. Stable and controlled crack growth occurs until ΔK_V reaches the fracture toughness value $\Delta K_C = (1-R)K_{IC}$ [2]. Figure 2c shows the range of fatigue crack growth for a plane Mixed Mode situation. Crack paths, which arise under these complex loadings will be described in the following sections.

EXPERIMENTAL INVESTIGATIONS OF CRACK GROWTH UNDER COMPLEX LOADING

For the pupose of experimental investigations of plane Mixed Mode problems several specimen types have already been proposed in the past. A summary is given in [3, 4]. Besides other ones in particular the CTS specimen [5, 6] with the appropriate loading device (Figure 3) has been established for Mixed Mode experiments. The loading

device allows to apply pure Mode I, pure Mode II, as well as five (or even more) Mixed Mode-loading situations to the CTS specimen by the use of just a uniaxial tension testing machine. For the purpose of varying the Mixed Mode-loading only the angle α has to be changed. Beginning from a starter notch at first a Mode I-fatigue crack has to be initiated in the CTS specimen. By alteration of the loading angle α afterwards the Mixed Mode experiment can be started. Thereby the crack grows into a new direction, which means, that by a sudden change of the loading direction the crack kinks under a specific angle φ_0 (Figure 4 and Figure 6).
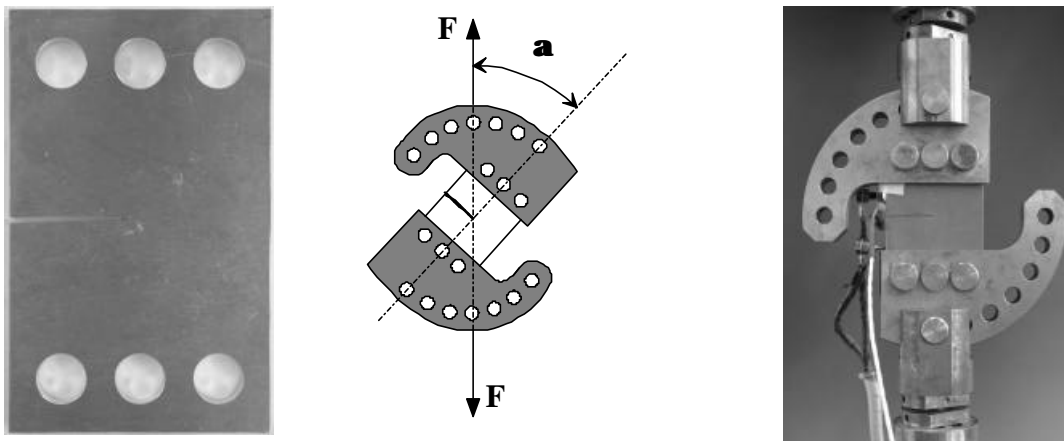
Figure 3. CTS-specimen and loading device for Mixed Mode fatigue crack growth tests.

Figure 4a shows a number of specimen with an increasing Mixed Mode-portion. The specimen in the front is loaded under $\alpha = 0°$ (Mode I, $\varphi_0 = 0°$), while the specimen in the back is loaded under $\alpha = 90°$ (Mode II, $\varphi_0 = 70°$). The complete crack path for a Mixed Mode situation ($\alpha = 75°$) is illustrated in Figure 4b.

a)

b)
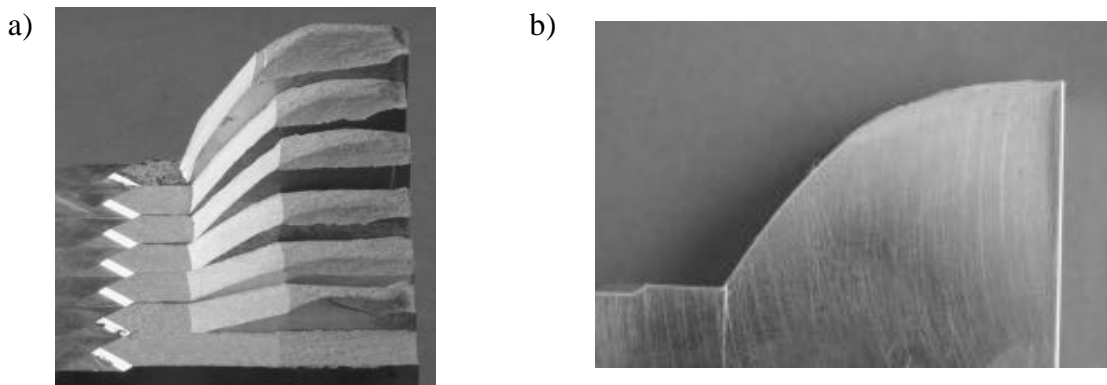
Figure 4. a) Fatigue crack paths under different Mixed Mode loading conditions
b) Crack paths in a CTS specimen with a loading direction $\alpha = 75°$
in an Aluminium alloy.

Figure 5 shows a branched crack, which results from a cyclic Mode II-fatigue loading with an R-ratio of –1. Such crack problems in practice i. a. occur in the web of railway lines. Due to asymmetrical geometries of the specimen or the component also a branched crack can be formed, which at the beginning features no sharp-edged crack (Figure 5b).

a)
b)
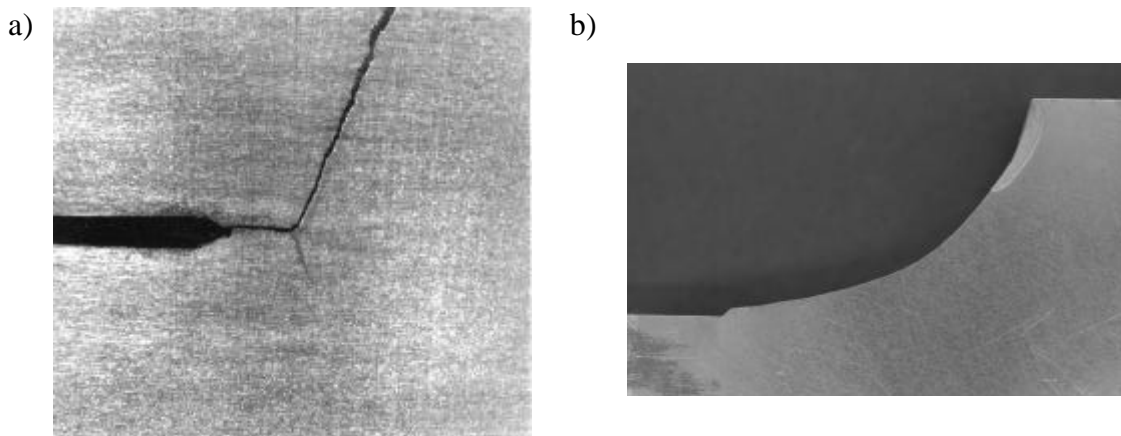
Figure 5. a) Branched crack under cyclic Mode II loading with a R-ratio of –1
b) Curved crack under a slight Mixed Mode loading.

The crack's kinking or deflection angle φ_0 as a function of the K_{II}/K_I-ratio resp. the $|K_{II}| / (|K_I| + |K_{II}|) = (K_{II}/K_I) / (1 + K_{II}/K_I)$-ratio is presented in Figure 6.
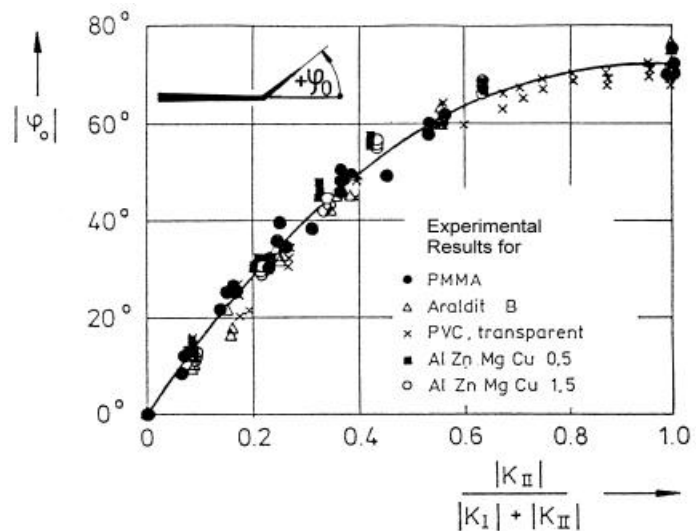
Figure 6. Measured crack deflection angles for different K_{II}/K_I-ratios and different materials.

It becomes apparent, that the angle φ_0 for isotropic or nearly isotropic materials only depends on the loading conditions at the crack tip and not on the particular material.

NUMERICAL SIMULATION OF FATIGUE CRACK GROWTH

For the numerical simulation of fatigue crack growth under plane Mixed Mode-loading several Finite-Element and Boundary-Element programs do exist. Within the scope of this paper the program FRANC/FAM, whose program architecture is illustrated in Figure 7, will be presented. In this program system the fatigue crack growth is realised by an incremental crack propagation, which is controlled by the stress intensities at the crack tip. The program takes into account the crack growth rate curve $da/dN = f(\Delta K_V)$ as well as the fracture mechanical limits ΔK_{th} and ΔK_C [9-11].

GEOMETRY, DESIGN	MATERIAL PROPERTIES	SERVICE LOAD	BOUNDARY CONDITIONS	CONTROL DATA
initial mesh, thickness, starter cracks	E, ν, $R_{p0.2}$, ΔK_{th}, ΔK_{Ic}, a, C, m	F_{max}, R	v_x, v_y	N_{end}, N_{max}, Δa_0

FRANC/FAM

PREPROCESSING

SIMULATION

AUTOMATIC ADAPTATION OF THE FE MESH	FINITE-ELEMENT ANALYSIS	FRACTURE MECHANICAL EVALUATION

POSTPROCESSING

STRESSES AND STRAINS	FRACTURE MECH. PROPERTIES	GEOMETRY DATA	FATIGUE DATA
σ_{ij}, σ_v, u_x, u_y	K_I, K_{II}, K_v, φ_0	coordinates of crack tip(s)	$\Delta K_v(a)$, $a(N)$, N_p, $da/dN(\Delta K_v)$, a_c

Figure 7. Finite-Element program for the simulation of fatigue crack growth.

The first simulation example for this program is a knee-lever, whose loading with a cyclic force $F(t)$ and displacements restraints can be gathered from Figure 8a. If only crack (a) is located in the knee-lever, this crack sharply kinks at the beginning of the simulation. In the following the crack grows slightly curved towards the border (Figure 8b). Before the kinking of the crack, a Mixed Mode loading situation with a high Mode II-portion at the crack tip is given. This high Mode II-portion is reduced during the simulation, before it increases again in the very near of the border. If only crack (c) is located in the knee-lever, the crack path shown in Figure 8c will develop. At the end of the simulation the knee-lever fails by instable crack growth under pure Mode I-loading. If otherwise all three cracks (a), (b) and (c) are arranged in the knee-lever, so only crack (b) and crack (c) will grow, whereby the shortest crack (b) is subjected to the highest

stress intensity. The propagation of crack (b) takes place under pure Mode I-loading up to the failure of the component.
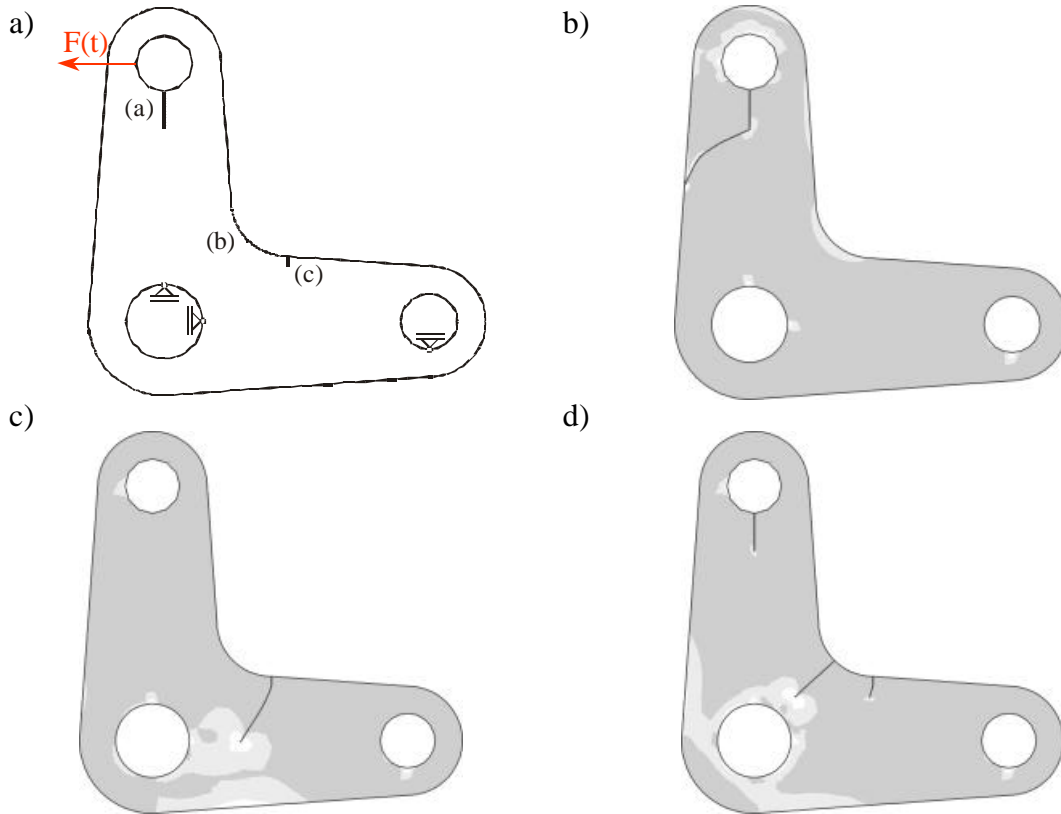
Figure 8. Simulated fatigue crack growth in a knee-lever
a) Geometry and loading
b) Crack path for crack (a)
c) Crack path for crack (c)
d) Crack paths for the three interacting cracks.

The crack growth of the structure in Figure 9 is mainly affected by a normal force N(t) and a shearing force Q(t). For the case, that only N(t) is applied, a crack path according to (1) is calculated. The second crack tip (on the right hand side) thereby is slightly bended towards the drilling hole. If the normal and the shearing force N(t) and Q(t) are superimposed in-phase, the crack sharply kinks at both starting crack tips as can be seen in crack path (2). If thirdly the normal and shearing force are of the same magnitude, a switch of the algebraic sign of the shearing force creates a totally different crack path (3). This behaviour places emphasis on the fact, that not only the absolute values of the stress intensities K_I and K_{II}, but also the algebraic sign of K_{II} is of importance for the path, that the crack takes [4].
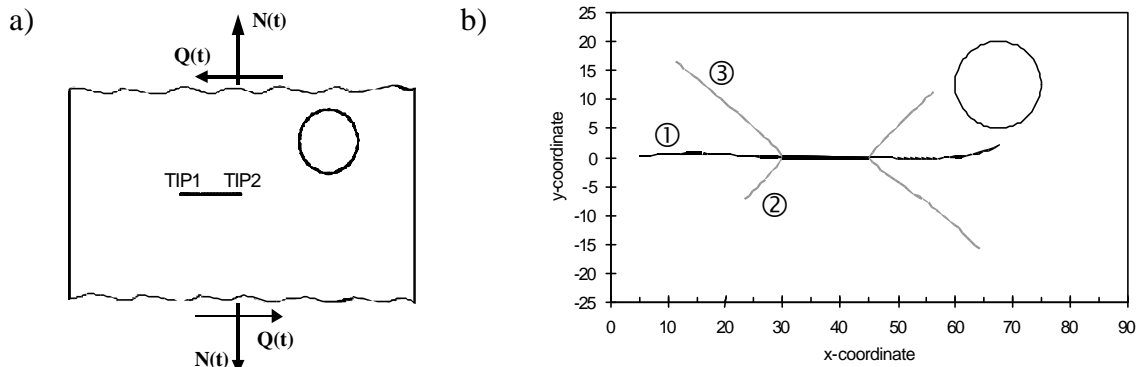
Figure 9. Simulated fatigue crack growth in a structure
a) Geometry and loading
b) Crack paths for different loading cases.

CONCLUSION

In this contribution fatigue crack paths under complex loading are determined by experimental as well as numerical simulations. Thereby for reasons of clarity only plane Mixed-Mode-situations are under consideration. However, also for 3D-Mixed-Mode-problems, which means the superposition of the fracture modes I, II and III, there do exist theoretical concepts [12, 13], specimen and loading devices for experiments [14] as well as numerical simulation codes [7, 8]

REFERENCES

1. Richard, H.A, Linnig, W. and Henn, K. (1991) *J. Forensic Engng.* **3**, 99.
2. Richard, H.A, Schöllmann, M., Fulland, M. and Sander, M. (2001) *Proc. of 6th Int. Conf. of Biaxial/Multiaxial Fatigue & Fracture*, Vol. **2**, 623-630.
3. Richard, H.A (1989) In: *Biaxial and Multiaxial Fatigue*, pp. 217-229, Brown, M.W., Miller, K.J (Eds.), Mechanical Engineering Publications, London.
4. Richard, H.A. (1985) *Bruchvorhersage bei überlagerter Normal- und Schubbeanspruchung von Rissen*, VDI-Verlag, Düsseldorf.
5. Richard, H.A. and Benitz, K., (1983) *Int. J. Frac.* **22**, R55/R58.
6. Richard, H.A. (1984) In: *Advances in Fracture Research*, pp. 3337-3344, Valluri, S.R. et al. (Eds.), Pergamon Press, Oxford.
7. Fulland, M., Schöllmann, M. and Richard, H.A. (2001) In: *CD-Rom Proceedings of ICF10*, Honolulu, USA.
8. Schöllmann, M., Fulland, M. and Richard, H.A. (2003) *Eng. Frac. Mech.* **70,** 249-268.
9. Erdogan, F. and Ratwani, M. (1970) *Int. J. Frac*. Mech. **6,** 379-392.
10. Schöllmann, M. and Richard, H.A. (1999) *J. Struct. Engng.* **26,** 39-48.

11. Richard, H.A. and Schöllmann, M. (1999) In: *Fatigue `99,* pp. 839-844, Wu, X.-R., Wang, Z.-G. (Eds.), Higher Education Press, Peking.
12. Schöllmann, M., Richard, H.A., Kullmer, G. and Fulland, M. (2002) *Int. J. Frac.* **117**, 129-141.
13. Richard, H.A., Schöllmann, M., Buchholz, F.G. and Fulland, M. (2003) In: *DVM-Bericht 235*, pp. 327-339, Deutscher Verband für Materialforschung und –prüfung e.V., Berlin.
14. Richard, H.A. (2001) In: *CD-Rom Proceedings of ICF10*, Honolulu, USA.